

Enhancing Heat Dissipation of Quantum Dots in High-Power White LEDs by Thermally Conductive Composites Annular Fins

Xuan Yang, Shuling Zhou, Bin Xie, Xingjian Yu, Xinfeng Zhang, Linyi Xiang, Kai Wang¹, Member, IEEE, and Xiaobing Luo², Fellow, IEEE

Abstract—In this work, QDs/hBNs/silicone annular fins (QDs-AF) are proposed as a new type of packaging structure to establish rapid heat dissipation pathways between QDs and heat sink. The QDs-AF structure was firstly designed based on commercial LEDs modules. Then, the annular fin materials including QDs, thermally conductive hBN platelets (hBNs), and silicone were determined by balancing the tradeoff of optical and thermal performances. Finally, the optimal structure of QDs-AF was obtained through thermal simulation by changing the values of fin thicknesses of different initial QDs-AF structures. According to the optimal QDs-AF structure with 4 fins and fin thickness of 0.28 mm, we fabricated the QDs-AF and its WLEDs. Compared with QDs-WLEDs, the maximum surface working temperature of QDs-AF-WLEDs was reduced by 20 °C at 1000 mA. In addition, the QDs-AF-WLEDs showed an excellent optical performance with a high color rendering index of 90.3 and a high luminous efficiency of 124.1 lm W⁻¹. The application of QDs-AF in WLEDs is a new and significant method to achieve a lower working temperature and protect QDs from thermal quenching in WLEDs.

Index Terms—High power, white LEDs, quantum dots, thermal management, fins.

I. INTRODUCTION

QUANTUM dots have received numerous attention in recent years due to their unique optical characteristics such as high luminous efficiency, narrow full-width at half maximum (FWHM), and tunable emission wavelength [1]–[3]. The WLEDs containing red-emissive quantum dots, blue-emissive chips, and yellow-emissive phosphor

(QDs-WLEDs) have achieved outstanding luminous efficiency (LE) and color rendering index (CRI), and become the most promising devices for lighting and display [4]–[6].

However, during the working process of QDs-WLEDs, the heat loss from QDs and phosphor hardly transfers out because they are embedded in silicone with ultralow thermal conductivity, which results in high working temperature of 150~200 °C [7] in the emitting layer. Zhao *et al.* found that colloidal QDs almost lost their luminous abilities when the temperature exceeded 150 °C [8]. The high temperature induces thermal quenching and quantum yield decrease toward QDs due to their thermal instability [9]. At present, reducing the working temperature of emitting layer has become a significant issue for the widespread application of QDs-WLEDs.

A lot of researches have been done to alleviate the high temperature problem in QDs-WLEDs. Some researches increased the thermal conductivity of emitting layer by incorporating the high thermal conductive hexagonal boron nitride platelets (hBNs) [10]–[13]. Especially, Xie *et al.* [10] fabricated the QDs/hBNs to raise the heat diffusion of QDs to decrease the maximum working temperature by 22.7 °C. New packaging structures of WLEDs were also proposed to reduce the QDs' working temperature [14]–[18]. Chen *et al.* prepared a remote spherical-shell QDs emitting layer [14] to separate QDs from the heat loss producer LEDs chip, and the maximum working temperature was decreased by 4.8 °C. On the other hand, Luo *et al.* directly coated silicon dioxide encapsulated QDs onto LEDs chip to form a QDs-on-chip packaging structure [16] to shorten the thermal resistance between QDs and heat sink under chip. However, these two package structures are challenging in the application of high-power WLEDs [19]. The remote QDs emitting layers possess a large thermal resistance and very limited thermal transfer path. As for the QDs-on-chip package, the situation is more severe since the more evident reabsorption effect.

To solve this issue, we proposed to establish efficient heat dissipation pathways between QDs and heat sink, by the QDs/hBNs/silicone annular fins (QDs-AF). With the incorporation of hBNs into the QDs/silicone, the QDs have more chance to contact with the high-thermal conductivity hBN platelets, thus their heat can be dissipated through the QDs-hBNs-silicone route and even QDs-hBNs-hBNs route. Therefore, the overall thermal dissipation performance is enhanced. The concentration of hBNs in QDs/silicone

Manuscript received May 28, 2021; accepted June 4, 2021. Date of publication June 10, 2021; date of current version July 26, 2021. This work was supported in part by the Ministry of Science and Technology of the People's Republic of China under Grant 2017YFE0100600, in part by the Open Project Program of Wuhan National Laboratory for Optoelectronics under Grant 2018WNLOKF017, in part by the China Postdoctoral Science Foundation under Grant 2020M672346, and in part by the National Natural Science Foundation of China under Grant 51625601. The review of this letter was arranged by Editor T.-Y. Seong. (Corresponding author: Xiaobing Luo.)

Xuan Yang, Shuling Zhou, Bin Xie, Xingjian Yu, Xinfeng Zhang, Linyi Xiang, and Xiaobing Luo are with the Wuhan National Laboratory for Optoelectronics, School of Energy and Power Engineering, Huazhong University of Science and Technology, Wuhan 430074, China (e-mail: luoxb@hust.edu.cn).

Kai Wang is with the Department of Electrical and Electronic Engineering, Southern University of Science and Technology, Shenzhen 518055, China.

Color versions of one or more figures in this letter are available at <https://doi.org/10.1109/LED.2021.3088280>.

Digital Object Identifier 10.1109/LED.2021.3088280

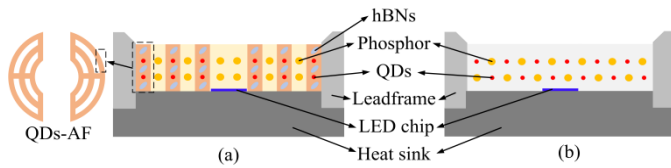


Fig. 1. Schematic of (a) QDs-AF-WLEDs and (b) conventional QDs-WLEDs.

TABLE I
THICKNESS AND THERMAL CONDUCTIVITY PARAMETERS FOR SIMULATION

Component	Thermal conductivity κ ($\text{W m}^{-1} \text{K}^{-1}$)	Height (mm)	Heat power (W)	Thickness (mm)
Heat sink	130	20	0	/
Leadframe	1	30	0	/
Blue LED chip	63	0.2	4.36	/
QDs-AF	0.274	1	0.22	0.18~0.38
Phosphor gel	0.182	1	0.26	0.0125~0.705

was determined by the opto-thermal tradeoff of hBNs. The structure of QDs-AF applied in 10 Watt input LEDs was optimized by thermal simulation. Fig. 1 shows the schematic of QDs-AF-WLEDs and QDs-WLEDs. Compared with traditional QDs-WLEDs, QDs-AF-WLEDs show an evidently lower working temperature than that of traditional QDs-WLEDs, with neglectable degradations in optical performance.

II. SIMULATION AND EXPERIMENT

A. Structure Design and Optimization of QDs-AF

We designed three initial structures of QDs-AF and attained the optimized structure parameters by thermal simulation using Comsol Multiphysics. The space between the two pieces is leaved for the LED chip and its bonding wire. Three initial structures had different numbers of annular fins: 3 fins with 2 interspaces (3F), 4 fins with 3 interspaces (4F) and 5 fins with 4 interspaces (5F). The fin thickness ranges from 0.18 mm to 0.38 mm. And the thicknesses of fins and interspaces are corelative.

Fig. 2a shows each component of the simulated QDs-AF-WLEDs. Their thickness and thermal conductivity for simulation are listed in Table. I. The thermal conductivity of the QDs-AF in the simulation was set as $0.274 \text{ W m}^{-1} \text{ K}^{-1}$ which is corresponded to the proper mass concentration of hBNs (15 wt%) in QDs-AF with acceptable optical performance decrease and obvious thermal performance increase. The thickness of phosphor gel is equal to the interspace width, ranging from 0.705 mm to 0.0125 mm with the increase of fin thickness.

The settings of the boundary conditions are as follows: the ambient temperature is constant at $25 \text{ }^\circ\text{C}$; convection heat transfer coefficient of bottom surface of sink is $245 \text{ W m}^{-2} \text{ K}^{-1}$; and natural convection heat transfer coefficient of other surfaces is $5 \text{ W m}^{-2} \text{ K}^{-1}$.

B. Fabrication of QDs-AF and Packaging for WLEDs

The fabrication process of QDs-AF and WLEDs are illustrated in Fig. 2b and Fig. 2c. For QDs-AF, red-emissive QDs (Poly OptoElectronics Ltd), hBNs (Momentive) with an average diameter of $19 \text{ }\mu\text{m}$ (the morphology is shown in inset

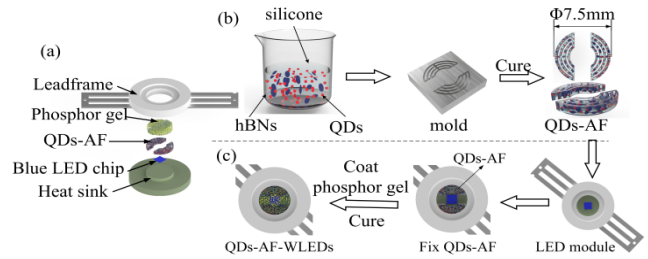


Fig. 2. (a) Schematics of the components in QDs-AF-WLEDs. (b) Fabrication of QDs-AF. (c) Fabrication of QDs-AF-WLEDs.

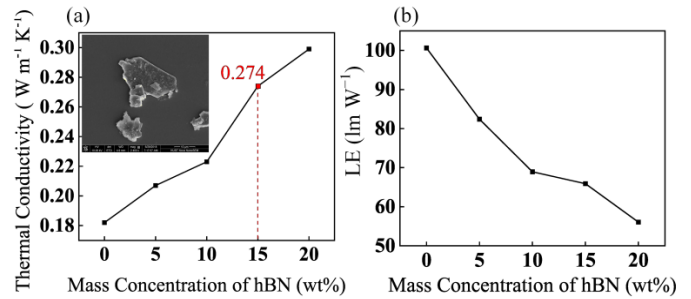


Fig. 3. (a) Thermal conductivities of different films. Inset is the morphology of hBNs. (b) LE of different films covered WLEDs.

of Fig. 3a) and silicone (Dow corning 184) were mixed, vacuumed and poured into the pre-processed mold of the optimized QDs-AF followed by heating to cure the mixture. Then QDs-AF was coated on LED model and filled with phosphor gel to fabricate the QDs-AF-WLEDs. For QDs-WLEDs, QDs, yellow-emissive phosphor (Intematix) and silicone were mixed and coated on LED module. After fabrication, optical performance and surface temperature of the above WLEDs were measured by an EVERFINE ATA-1000 Auto-temperated LED Opto-electronic Analyzer and a FLIR SC620 infrared thermal imager, respectively.

III. RESULT AND DISCUSSION

A. Optimized Structure of QDs-AF

Five hBNs/silicone films with different mass concentrations (0 wt% (pure silicone) ~ 20 wt%) of hBNs were fabricated. We measured their thermal conductivity and covered the films on a WLEDs to compare the LE loss. The results are shown in Fig. 3. We found that the hBNs/silicone film with 15 wt% of hBNs had the largest thermal conductivity enhancement and lowest LE loss of per one wt% of hBNs. Therefore, we finally chose the mass concentration of 15 wt% for hBNs.

Fig. 4a shows the simulative maximum working temperature curves of QDs-AF-WLEDs with different initial structures and fin thicknesses. It has been mentioned that when the fin thickness increases, the interspace width decreases under the same number of fins. As the fin thickness increases, the contact area between the QDs-AF and the heat sink increases, enhancing the conduction from the QDs-AF to heat sink. However, when the fin is too thick, the interspace width becomes too small, leading to high heat density of the phosphor gel, which results in temperature rise. So, there is an optimal fin thickness of the QDs-AF to achieve a lowest temperature. The lowest maximum temperatures and related fin thicknesses were $125.4 \text{ }^\circ\text{C}$ and 0.36 mm for 3-fins (3F) QDs-AF-WLEDs,

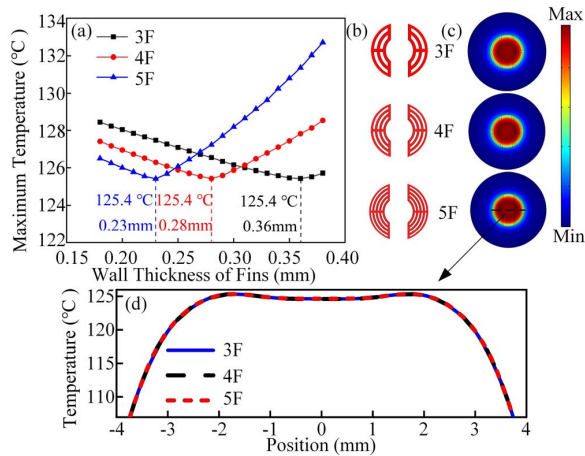


Fig. 4. (a) Maximum temperatures corresponding to fin thicknesses of different initial structures. (b) Three optimal structures. (c) Temperature distributions of three optimal structures. (d) Temperature distribution curves of the emitting layer.

125.4 °C and 0.28 mm for 4F one, 125.4 °C and 0.23 mm for 5F one. Three optimal structures with different numbers of fins are shown in Fig. 4b. The 4-fins QDs-AF with a fin thickness of 0.28 mm was demonstrated to be the best one to apply in WLEDs for the following reasons: In optics, there are more QDs gathering in each single annular fin of the 3F compared to the others, which may increase the light reabsorption among the QDs, causing more light loss. In processing, the interspace width is only 0.2 mm of the 5F, which is unpractical for processing (interspace width needs to be larger than 0.25 mm) while that of 4F is large enough as 0.28 mm.

B. Thermo-Optic Performance of QDs-WLEDs

The insets in Fig. 5a show the fabricated 4-fins QDs-AF under day light (left) and UV light (right) irradiation, respectively. The packaged QDs-WLEDs and QDs-AF-WLEDs are shown in Fig. 5b and connected in series to be under the same driving currents. Fig. 5a shows the maximum surface working temperature curves of QDs-WLEDs and QDs-AF-WLEDs with increasing driving currents. QDs-AF-WLEDs showed much lower temperatures comparing with QDs-WLEDs under the same driving currents. In detail, the maximum surface working temperatures of QDs-AF-WLEDs were lower than that of QDs-WLEDs by 1.4, 11.5 and 20 °C at 100, 600 and 1000 mA, respectively, as shown in Fig. 5c-d. The temperature drops enlarged with the increasing driving current, implying the application potential of QDs-AF in higher-power WLEDs.

The optical performances of QDs-AF-WLEDs and QDs-WLEDs were also measured. As shown in Fig. 6a, the two WLEDs exhibited similar spectra under driving current of 20 mA. Furthermore, Fig. 6b-d provide the CRI, LE, and CCT curves with increasing driving currents. Under 20 mA, QDs-AF-WLEDs and QDs-WLEDs showed high CRI of 90.3 and 91, high LE of 124.1 and 131.8 lm W⁻¹, CCT of 5536 and 5315 K, and similar CIE coordinates of (0.3318, 0.3646) and (0.3377, 0.3695) shown in the inset of Fig. 6d, respectively. The scattering effect of hBNs causes light loss resulting in the lower LE of QDs-AF-WLEDs. The red light scattering by hBNs increases the reabsorption of

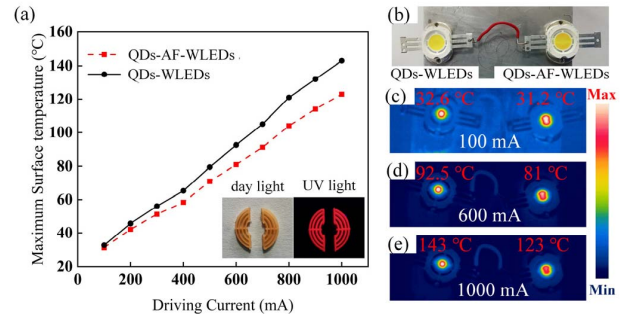


Fig. 5. (a) Maximum surface temperatures of QDs-WLEDs and QDs-AF-WLEDs with increasing driving currents. Insets are the QDs-AF under day light and UV light. (b) QDs-WLEDs and QDs-AF-WLEDs in series and their steady-state temperature distributions at (c) 100 mA, (d) 600 mA and (e) 1000 mA.

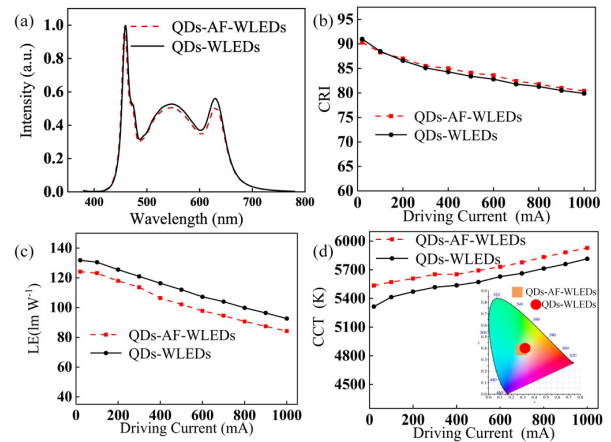


Fig. 6. (a) Spectra of QDs-AF-WLEDs and QDs-WLEDs under driving current of 20 mA. (b) CRI, (c) LE and (d) CCT of the WLEDs varies with driving currents. Inset is the CIE coordinates of the WLEDs at 20 mA.

red light by QDs resulting in the higher CCT. In addition, QDs-AF-WLEDs showed similar optical performance tendency with that of QDs-WLEDs under the increasing driving currents. Above similarities proved that the package structure in QDs-AF-WLEDs had neglectable effect to their optical performance.

IV. CONCLUSION

We designed a new LED package structure to enhance the heat dissipation of QDs-WLEDs. The proposed QDs/hBNs/silicone annular fin (QDs-AF) established rapid heat dissipation pathways between QDs and heat sink. Through simulation and opto-thermal tradeoff of hBNs, the optimal QDs-AF structure had 4 fins with a thickness of 0.28 mm and mass concentration of hBNs is 15 wt%. QDs-AF-WLEDs showed better thermal performance than QDs-WLEDs under increasing driving currents. The maximum surface working temperature of QDs-AF-WLEDs was 20 °C lower than QDs-WLEDs at 1000 mA. Meanwhile, the QDs-AF-WLEDs still maintained excellent optical performance: LE of 124.1 lm W⁻¹, CRI of 90.3. Overall, as a new type of LED packaging, QDs-AF provides a novel method to both achieve considerable enhancement in thermal performance and maintain optical performance. Featuring simple fabrication process and excellent opto-thermal performance, the QDs-AF will facilitate the thermal management and wide application of QDs-WLEDs.

REFERENCES

- [1] D. V. Talapin and J. Steckel, "Quantum dot light-emitting devices," *MRS Bull.*, vol. 38, no. 9, pp. 685–691, Sep. 2013, doi: [10.1557/mrs.2013.204](https://doi.org/10.1557/mrs.2013.204).
- [2] Y.-H. Won, O. Cho, T. Kim, D.-Y. Chung, T. Kim, H. Chung, H. Jang, J. Lee, D. Kim, and E. Jang, "Highly efficient and stable InP/ZnSe/ZnS quantum dot light-emitting diodes," *Nature*, vol. 575, no. 7784, pp. 634–638, Nov. 2019, doi: [10.1038/s41586-019-1771-5](https://doi.org/10.1038/s41586-019-1771-5).
- [3] B. Xie, R. Hu, and X. Luo, "Quantum dots-converted light-emitting diodes packaging for lighting and display: Status and perspectives," *J. Electron. Packag.*, vol. 138, no. 2, Apr. 2016, Art. no. 020803, doi: [10.1115/1.4033143](https://doi.org/10.1115/1.4033143).
- [4] H. C. Kim, H.-G. Hong, C. Yoon, H. Choi, I.-S. Ahn, D. C. Lee, Y.-J. Kim, and K. Lee, "Fabrication of high quantum yield quantum dot/polymer films by enhancing dispersion of quantum dots using silica particles," *J. Colloid Interface Sci.*, vol. 393, pp. 74–79, Mar. 2013, doi: [10.1016/j.jcis.2012.10.045](https://doi.org/10.1016/j.jcis.2012.10.045).
- [5] M.-H. Shin, H.-G. Hong, H.-J. Kim, and Y.-J. Kim, "Enhancement of optical extraction efficiency in white LED package with quantum dot phosphors and air-gap structure," *Appl. Phys. Exp.*, vol. 7, no. 5, Apr. 2014, Art. no. 052101, doi: [10.7567/apex.7.052101](https://doi.org/10.7567/apex.7.052101).
- [6] B. Xie, R. Hu, X. Yu, B. Shang, Y. Ma, and X. Luo, "Effect of packaging method on performance of light-emitting diodes with quantum dot phosphor," *IEEE Photon. Technol. Lett.*, vol. 28, no. 10, pp. 1115–1118, May 15, 2016, doi: [10.1109/lpt.2016.2531794](https://doi.org/10.1109/lpt.2016.2531794).
- [7] V. Bachmann, C. Ronda, and A. Meijerink, "Temperature quenching of yellow Ce³⁺ luminescence in YAG:Ce," *Chem. Mater.*, vol. 21, no. 10, pp. 2077–2084, May 2009, doi: [10.1021/cm8030768](https://doi.org/10.1021/cm8030768).
- [8] Y. Zhao, C. Riemersma, F. Pietra, R. Koole, C. de Mello Donegá, and A. Meijerink, "High-temperature luminescence quenching of colloidal quantum dots," *ACS Nano*, vol. 6, no. 10, pp. 9058–9067, Sep. 2012, doi: [10.1021/nn303217q](https://doi.org/10.1021/nn303217q).
- [9] K.-J. Chen, H.-C. Chen, M.-H. Shih, C.-H. Wang, M.-Y. Kuo, Y.-C. Yang, C.-C. Lin, and H.-C. Kuo, "The influence of the thermal effect on CdSe/ZnS quantum dots in light-emitting diodes," *J. Lightw. Technol.*, vol. 30, no. 14, pp. 2256–2261, Jul. 2012, doi: [10.1109/jlt.2012.2195158](https://doi.org/10.1109/jlt.2012.2195158).
- [10] B. Xie, H. Liu, R. Hu, C. Wang, J. Hao, K. Wang, and X. Luo, "Targeting cooling for quantum dots in white QDs-LEDs by hexagonal boron nitride platelets with electrostatic bonding," *Adv. Funct. Mater.*, vol. 28, no. 30, Jul. 2018, Art. no. 1801407, doi: [10.1002/adfm.201801407](https://doi.org/10.1002/adfm.201801407).
- [11] Y. Xie, D. Yang, L. Zhang, Z. Zhang, C. Geng, C. Shen, J. G. Liu, S. Xu, and W. Bi, "Highly efficient and thermally stable QD-LEDs based on quantum Dots-SiO₂-BN nanoplate assemblies," *ACS Appl. Mater. Interfaces*, vol. 12, no. 1, pp. 1539–1548, Jan. 2020, doi: [10.1021/acsami.9b18500](https://doi.org/10.1021/acsami.9b18500).
- [12] H. Zheng, X. Lei, T. Cheng, S. Liu, X. Zeng, and R. Sun, "Enhancing the thermal dissipation of a light-converting composite for quantum dot-based white light-emitting diodes through electrospinning nanofibers," *Nanotechnology*, vol. 28, no. 26, Jun. 2017, Art. no. 265204, doi: [10.1088/1361-6528/aa72d6](https://doi.org/10.1088/1361-6528/aa72d6).
- [13] S. Zhou, B. Xie, Y. Ma, W. Lan, and X. Luo, "Effects of hexagonal boron nitride sheets on the optothermal performances of quantum dots-converted white LEDs," *IEEE Trans. Electron Devices*, vol. 66, no. 11, pp. 4778–4783, Nov. 2019, doi: [10.1109/ted.2019.2937340](https://doi.org/10.1109/ted.2019.2937340).
- [14] S. Chen, C. Yan, Y. Tang, J. Li, X. Ding, L. Rao, and Z. Li, "Improvement in luminous efficacy and thermal performance using quantum dots spherical shell for white light emitting diodes," *Nanomaterials*, vol. 8, no. 8, p. 618, Aug. 2018, doi: [10.3390/nano8080618](https://doi.org/10.3390/nano8080618).
- [15] Z.-T. Li, J.-X. Li, J.-S. Li, X.-W. Du, C.-J. Song, and Y. Tang, "Thermal impact of LED chips on quantum dots in remote-chip and on-chip packaging structures," *IEEE Trans. Electron Devices*, vol. 66, no. 11, pp. 4817–4822, Nov. 2019, doi: [10.1109/ted.2019.2941911](https://doi.org/10.1109/ted.2019.2941911).
- [16] B. Xie, H. Liu, X. W. Sun, X. Yu, R. Wu, K. Wang, and X. Luo, "Reduced working temperature of quantum dots-light-emitting diodes optimized by quantum dots at silica-on-chip structure," *J. Electron. Packag.*, vol. 141, no. 3, Apr. 2019, Art. no. 031001, doi: [10.1115/1.4042981](https://doi.org/10.1115/1.4042981).
- [17] D. Yang, Y. Xie, C. Geng, C. Shen, J. G. Liu, M. Sun, S. Li, W. Bi, and S. Xu, "Thermal analysis and performance optimization of quantum dots in LEDs by microsphere model," *IEEE Trans. Electron Devices*, vol. 66, no. 9, pp. 3896–3902, Sep. 2019, doi: [10.1109/ted.2019.2930898](https://doi.org/10.1109/ted.2019.2930898).
- [18] Z.-T. Li, C.-J. Song, Q.-L. Zhao, J.-S. Li, J.-L. Zheng, and Y. Tang, "Study on the separation packaging structure of quantum dot-phosphor hybrid white light-emitting diodes for backlight display," *IEEE Trans. Compon., Packag., Manuf. Technol.*, vol. 10, no. 7, pp. 1204–1211, Jul. 2020, doi: [10.1109/TCPMT.2020.2998541](https://doi.org/10.1109/TCPMT.2020.2998541).
- [19] J.-S. Li, Y. Tang, Z.-T. Li, G.-W. Liang, X.-R. Ding, and B.-H. Yu, "High thermal performance and reliability of quantum-dot-based light-emitting diodes with watt-level injection power," *IEEE Trans. Device Mater. Rel.*, vol. 19, no. 1, pp. 120–125, Mar. 2019, doi: [10.1109/tdmr.2018.2886299](https://doi.org/10.1109/tdmr.2018.2886299).